Journal of Materials Chemistry C

Ferroelectricity of Poly(vinylidene fluoride) Homopolymer Langmuir–Blodgett Nanofilms

Journal:	*Journal of Materials Chemistry C*
Manuscript ID:	TC-COM-03-2014-000600.R1
Article Type:	Communication
Date Submitted by the Author:	04-Jun-2014

Complete List of Authors:	Zhu, Huie; Tohoku University, IMRAM Yamamoto, Shunsuke; Tohoku University, IMRAM Matsui, Jun; Yamagata University, Miyashita, Tokuji; Tohoku University, Institute of Multidisciplinary Research for Advanced Materials Mitsuishi, Masaya; IMRAM, Tohoku University,

Ferroelectricity of Poly(vinylidene fluoride) Homopolymer Langmuir–Blodgett Nanofilms

Huie Zhu,[a] Shunsuke Yamamoto,[a] Jun Matsui,[b] Tokuji Miyashita,[a] Masaya Mitsuishi*[a]

[a]*Institute of Multidisciplinary Research for Advanced Materials (IMRAM), Tohoku University, 2-1-1 Katahira, Aoba-ku, Sendai 980-8577, Japan. E-mail: masaya@tagen.tohoku.ac.jp*

[b]*Department of Material and Biological Chemistry, Faculty of Science, Yamagata University, Kojirakawamachi 1-4-12, Yamagata 990-560, Japan.*

As-deposited poly(vinylidene fluoride) (PVDF) Langmuir–Blodgett (LB) nanofilms with complete β phase show remarkably high remanent polarization (P_r), about 6.6 μC/cm^2 at 81 nm. Extrinsic switching characteristics of the nanofilms are demonstrated. Results also show that highly oriented PVDF homopolymer LB nanofilms down to 12 nm with no post-treatment retain robust room-temperature ferroelectric polarization switching that is greater than 10^5 operation cycles, with longer standing fatigue endurance than those of PVDF copolymer nanofilms.

The increasing demand for flexible electronics has stimulated intense research on new nonvolatile memory devices based on functional polymers because of their versatile functionality, high mechanical flexibility, and easy processing for thin films.[1] For example,

functional polyimides containing aromatic moieties such as triphenylamine in main chain or in side chain have been of greatly interest because of their resistive switching behavior under electrical sweeps for nonvolatile memory devices.[2] Composites of conjugated polymer polyaniline with gold nanoparticles or silica show electrically or magnetically programmable bistability, which are also applicable for nonvolatile memory devices.[3] Besides functional conjugated polymers, ferroelectric polymers are another candidate for memory applications.[4]

Because of good ferroelectricity, low processing temperature, easy fabrication of thin film, and high flexibility, semicrystalline poly(vinylidene fluoride) (PVDF) based polymers are extremely attractive for non-volatile memories.[4c, 5] PVDF materials have at least five phases: α, β, γ, δ, and ε phases. Polar crystals, especially β-phase crystals, have an arrangement of PVDF molecules with all-trans conformations devoted to piezoelectric, pyroelectric, and ferroelectric properties of PVDF-based materials.[6] Usually in ferroelectric memories, information is stored in two antiparallel polarization states coded "0" or "1". A long-term bi-stable polarization state is rather critical for memory applications of polymer ferroelectric materials. That state is usually dependent on the film properties of β-phase PVDF. In other words, a high content of β crystals as well as high film regularity is necessary to achieve a high remanent polarization value (P_r), thereby eliciting good ferroelectric properties. However, low-voltage operations should be achieved. Decreasing the ferroelectric material thickness is generally a good choice because ferroelectrics switch at a threshold

electric field, the coercive field (E_c).[5] Many studies have been conducted to obtain poly(vinylidene fluoride-*co*-trifluoroethylene), P(VDF-TrFE)-based ferroelectric nanoscale materials, including spin-coating, nanoembossing,[4b] imprinting,[7] nanoconfinement,[8] and Langmuir–Schaefer (LS) technique[9] because the introduction of copolymerization units of TrFE creates a crystallization nucleus that is beneficial for high crystallinity. In contrast to PVDF copolymers, PVDF homopolymer presents numerous benefits for applications, such as easier synthesis, higher dipole density and higher thermal stability attributable to its high transition temperature (T_C) of about 170 °C.[10] Moreover, current leakage is suppressed in PVDF homopolymer thin films compared to that in PVDF copolymer thin films because of the current leaking path formed by the crystal defects of TrFE copolymerization units.[11] However, preparations and applications of high-performance PVDF homopolymer nanofilms have lagged behind those of copolymers. These results from low contents of β crystals and crystallinity were obtained using traditional methods such as spin-coating. Because of limitations attributable to ineffective film preparation, studies related to polarization switching characteristics and kinetics of PVDF homopolymer ultrathin films have rarely been conducted. Recently, we found that PVDF homopolymer can form a quasi-monolayer (about 2.31 nm) at the air–water interface, which can be transferred effectively onto various substrates by the addition of a miniscule amount of poly(*N*-dodecylacrylamide) (pDDA), an excellent amphiphilic polymer.[12] FT-IR measurements demonstrated that the contents of β

crystals in the PVDF LB nanofilms reached 95%, one of the highest values ever reported. The total crystallinity was kept as high as 50%, which is comparable to that of bulk PVDF. In addition, by controlling the deposited layer numbers, film thicknesses can be tuned freely by several nanometers. That tuning presents new opportunities for studying the application properties of PVDF homopolymer nanofilms for non-volatile nanomemories.

For this study, ferroelectric nanocapacitors (FeNCs) made of as-deposited PVDF homopolymer LB nanofilms were fabricated with different film thicknesses of 12–81 nm. The PVDF homopolymer quasi-monolayers were deposited from the air–water interface to the Al-coated glass substrates to the desired thicknesses, as described elsewhere.[12c] Polarization hysteresis loops were measured in FeNCs of different film thicknesses. The thickness-dependence of ferroelectricity of the PVDF LB nanofilms was also characterized. Films with thickness greater than 58 nm show a marked increase of P_r from 1.7 (12 nm) to 6.6 μC/cm^2 (81 nm), which is one of the highest values ever reported for PVDF homopolymer nanofilms. An as-deposited film as thin as 12 nm with no post-treatment was demonstrated as ferroelectric. This is the first report of ferroelectricity detection in such a thin PVDF homopolymer film. The film is also useful to ascertain the fatigue endurance properties of the PVDF FeNCs as a result of its good film properties.

PVDF (Aldrich, $M_n = 7.1 \times 10^4$, $M_w/M_n = 2.5$) LB nanofilms were prepared at 20 °C according to the reported method with different numbers of layers of 5–35 layers. Although

the film thickness can be easily tuned from several to several hundred nanometers, we just focus on the ultrathin films (< 100 nm) in this study because of their promising low-voltage operation.[12c] They have thicknesses of 12 nm (5 layers), 35 nm (15 layers), 58 nm (25 layers), and 81 nm (35 layers).[12c] Top and bottom Al electrodes (40 ± 5 nm) with area of 3 mm × 3 mm were thermally evaporated through a metal mask at a rate of 1.0 Å/s onto glass substrates for bottom electrodes and LB nanofilms for top electrodes. The samples were cooled using liquid nitrogen at 77 K during the deposition of top Al electrodes. The Fourier transform infrared (FT-IR) spectra were measured at a spectral resolution of 4 cm^{-1} using FT-IR (FT-IR 4200; Jasco Corp.) under a nitrogen atmosphere. Displacement (*D*)-electric field (*E*) hysteresis loops were characterized using a traditional Sawyer–Tower method with a triangle waveform voltage at a frequency of 10 Hz with a reference capacitor of 1 μF.[13]

The crystal structures of PVDF films are important for its application. As reported, well-known peaks at 763, 795, and 976 cm^{-1} are assigned to non-polar α crystals (Form II). The β crystal (Form I) is associated with absorptions at 840, 1276, and 1402 cm^{-1}, whereas the peak at 1233 cm^{-1} is characteristic for the γ crystal (Form III).[12c] **Figure 1(a)** shows FT-IR spectra of PVDF LB nanofilms on silicon substrates of different thicknesses. The dominant β crystals (Form I) in the 12-nm-thick film show that the air–water interface in LB technique is effective for obtaining polar crystals. When increasing the film thickness from 12 nm to 81 nm, β-crystal peaks become more outstanding. The absorbance of β crystals at 1276 and 840

cm^{-1} is shown as a function of number of layers in **Figures 1(b)** and **1(c)**. As the figures show, absorbance of these two spectral regions is increased by the linear relation to the film thicknesses. The linear relation implies good uniformity of PVDF LB nanofilm deposition. The uniform film structure can be further proved by the linear relations between the film thickness and the absorbance at 1185 cm^{-1} ($\nu_a(CF_2)$) and 1071 cm^{-1}($\nu_a(CC)$) in Figure S1, which has an absorption coefficient reasonably independent of the crystalline phase of PVDF and only dependent of the film thickness.[14]

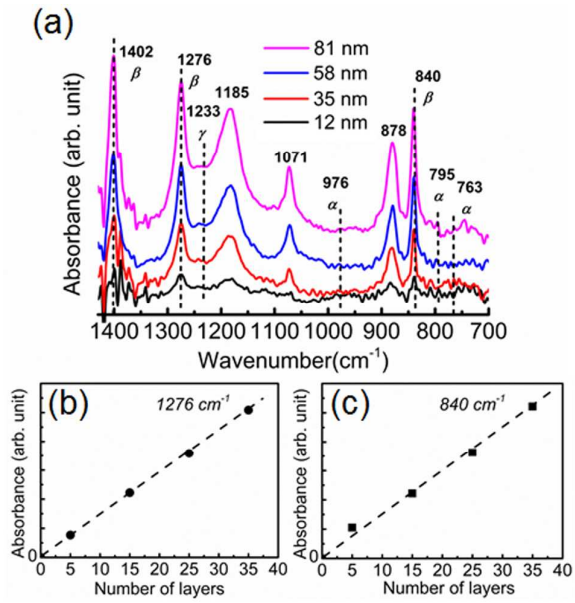

Figure 1. (a) FT-IR spectra of PVDF LB nanofilms on hydrophilic silicon substrates and their absorbance at (b) 1276 and (c) 840 cm^{-1} as a function of the number of layers.

The fractions of β crystals are obtainable using the following equation, assuming only that α and β crystals can be found in the PVDF LB nanofilms.[15]

$$F(\beta) = \frac{A_\beta}{\left(\frac{K_\beta}{K_\alpha}\right)A_\alpha + A_\beta}, \qquad (1)$$

Therein, A_β and A_α represent the absorbance of α, and β crystals at 766 and 840 cm^{-1}. K_α and K_β are the absorption coefficient at respective wavenumber, which are, respectively, 6.1×10^4 and 7.7×10^4 cm^2/mol. The calculated $F(\beta)$ values for 12-, 35-, 58- and 81-nm thick films are, respectively, 95.3%, 97.0%, 100% and 99.9%. These are the highest values ever reported for PVDF nanofilms. For a PVDF β crystal with an orthorhombic structure, our previous report described that the *b* axis (the molecular dipole) is extensively parallel to the substrate surface and that the *a* axis is perpendicular to substrate surface.[12c] For the present study, we demonstrate that the crystal orientation changes with the film thicknesses by comparing the value of A_{840}/A_{878} because the vibrational modes at 840 and 878 cm^{-1} respectively represent the symmetric stretching mode of CF_2 parallel to the *b* axis and the asymmetric stretching mode of CF_2 parallel to the *a* axis. The A_{840}/A_{878} values for 12-, 35-, 58- and 81-nm thick films are 0.60, 0.72, 1.00, and 0.97, respectively, which is indicative of more-parallel orientation of the *b* axis (polarization direction) in the thicker films.

The ferroelectric properties of the obtained FeNCs were measured using a Sawyer–Tower circuit produced in our laboratory. **Figure 2(a)** shows ferroelectric hysteresis loops measured at different film thicknesses at 10 Hz. Films with thickness of 81 nm show remanent polarization (P_r) of 6.6 $\mu C/cm^2$, which is one of the highest values ever reported for

PVDF homopolymer micro-/nanofilms.[16] This high value is attributable to the good film properties. Hysteresis loops with a narrow and unsaturated shape for the 12-nm PVDF LB nanofilm were also observed, which indicates that a film as thin as 12 nm is still ferroelectric. This report is the first to describe detection of ferroelectricity in such a thin PVDF homopolymer film. **Figure 2(b)** presents P_r values measured for films of different thicknesses. They are 1.7, 2.0, 5.3, and 6.6 μC/cm^2, respectively, for 12-, 35-, 58-, and 81-nm thick films. The decrease of P_r has been reported as resulting from a reduction of crystallinity and ferroelectric crystals with decreasing film thickness below 100 nm in spin-coated P(VDF-TrFE) films.[17] Another group also observed decreasing P_r with decreasing film thickness. That group inferred that the decrease originates from the metal–organic interfacial effects for Al electrodes.[18] The PVDF LB nanofilms deposited layer-by-layer have uniformly regular layer structures without thickness-dependent β-crystal contents, as the FT-IR spectra show. Therefore, it is reasonable to infer that the thickness-dependent P_r results from the metal–organic interfacial effect between the Al electrodes and the PVDF LB nanofilms. The marked increase of P_r for films with thicknesses exceeding 58 nm indicates that the interfacial effect on the ferroelectricity of the PVDF LB nanofilms has critical length of less than 58 nm, which shows good agreement with the value of 50 nm reported by Nakajima *et al*.[18-19]

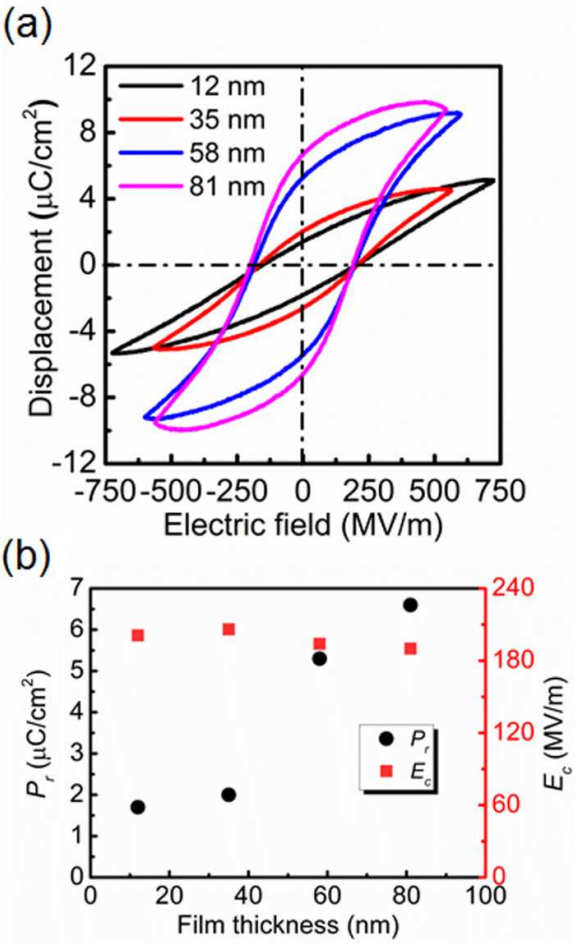

Figure 2. (a) Hysteresis loops and (b) remanent polarization (P_r) and coercive field (E_c) of PVDF LB nanofilms at different film thicknesses.

Polarization switching processes are classified as either intrinsic or extrinsic switching. For intrinsic switching, the ferroelectric crystal switches homogeneously by the collective rotation of the dipole without domain formation.[10] This happens only in the case of crystals that are thinner than the diameter of a critical nucleus. Therefore, the minimum size is necessary for domain growth. However, extrinsic switching is an inhomogeneous process involving domain nucleation and growth.[10, 20] Li *et al.* reported extrinsic switching of ferroelectric δ-PVDF ultrathin films down to 18 nm, which shows P_r and E_c that are

independent of the film thickness.[10] Similarly, the values of E_c for the FeNCs in this study, approximately 195 MV/m, are almost independent of the film thickness, as shown in **Figure 2(b)**. Those values are representative of the extrinsic switching characteristics of the PVDF LB nanofilms. Nakajima *et al.* demonstrated intrinsic switching using devices with inert Au electrodes.[18] Ducharme *et al*. observed that the switching mechanism is changed on the film thicknesses of PVDF copolymer Langmuir–Schaefer nanofilms.[20] They reported that a 54-nm-thick film exhibits extrinsic nucleation and domain-growth type kinetics, which is qualitatively different from an 18-nm-thick film, which exhibits intrinsic switching kinetics. Therefore, it is also possible to observe the intrinsic switching of PVDF homopolymer LB nanofilms using suitable electrodes at a critical film thickness, which will be studied further.

The breakdown strength of PVDF homopolymer LB nanofilms exceeds 500 MV/m, as shown in **Figure 2(a)**. This value is much higher than that of bulk PVDF (about 300 MV/m).[21] That fact indicates that PVDF LB nanofilms have good electric stability. It has been proved that the breakdown strength of polymer dielectrics generally increases concomitantly with decreasing film thickness.[22] An oxidized layer of Al_2O_3 on the electrode surface prevents current leakage, even for sub-10-nm thick films.[18] The existing Al_2O_3 layer in the surface of electrodes will affect the effective electric field (E_{eff}) applied at the ferroelectric films. The relation between E_{eff} and film thickness (d) can be expressed as [19, 23]

$$E_{eff} = -\frac{d_s}{d}\frac{P}{\varepsilon} + E, \qquad (2)$$

where d_s, P, ε, and E respectively represent the dead layer thickness, polarization, permittivity and the applied electric field. The first term on the right side of the equation expresses the depolarization field caused by the uncompensated surface polarization charge. During LB film deposition, the bottom Al electrodes were kept in contact with water, which might result in the formation of thicker Al_2O_3 dead layers. Therefore, the larger value of d_s/d induces a higher depolarization electric field, which explains the high breakdown strength of the PVDF homopolymer LB nanofilms.

Finally, we investigated polarization fatigue, which has not been studied, especially in PVDF homopolymer LB nanofilms. **Figure 3** shows the fatigue properties of FeNCs at different film thicknesses measured using a continuous triangular voltage at a frequency of 100 Hz. With the increasing number of polarization switching cycles, P_r values decreased gradually, exhibiting a trend that is similar to those of PVDF copolymer microfilms and LS nanofilms.[13a, 24] All films from 12 to 81 nm showed long-standing fatigue endurance exceeding 10^5 cycles. In the case of the 81-nm-thick PVDF homopolymer film, 10^6 cycle switching causes only 37% loss of the P_r value. This is lower than that of a 69-nm-thick P(VDF-TrFE) copolymer film. The P_r value reduces 50% of its initial value under 150 MV/m, 1 kHz after 10^6 cycles.[24] The PVDF homopolymer LB nanofilms in this study occupy a lower fatigue rate than copolymers do. This result might come from the absence of crystal defects in PVDF homopolymer introduced by the copolymerization repeating unit in copolymers, such

as trifluoroethylene (TrFE).[11] Such crystal defects usually act as a current leaking path during operation, engendering a high fatigue rate. In addition, the thinner the film is, the slower the fatigue rate becomes: 22% decrease of the initial polarization in the 12-nm FeNCs because the heat generated during polarization switching process diffuses quickly out of the thin films.[24] Good fatigue characteristics of the PVDF LB nanofilms make them very promising for actual applications. As reported, the fatigue rate of PVDF films is usually dependent on the frequency: higher fatigue rates are observed at lower frequencies.[13a] Therefore, our capacitors made of as-prepared PVDF homopolymer LB nanofilms can be operated at more cycles and show better fatigue properties under higher frequency such as 1 kHz, which have not been measured because of the restrictions of our measurement instruments.

The main mechanism of polarization fatigue is the inhibition of seeds of the opposite domain nucleation caused by the near-by electrode injection of space charges.[13a] The 35-nm and 81-nm thick films show a sudden onset decrease of polarization respectively from 10^4 and 10^3 switching cycles, which is expected to be related to high surface roughness, as shown in **Figure 4**. It is much easier for space charge injection to occur in a rougher surface. Furthermore, precise control of the thickness of Al_2O_3 layers on the electrodes of each device is difficult because the thickness is measured in an ambient atmosphere, thereby leading to highly uncertain influences on space charge injection and the irregular change of fatigue curves with film thicknesses. Furthermore, the molecular orientation changes according to the

film thickness, as discussed before, which might also affect the measurement results.

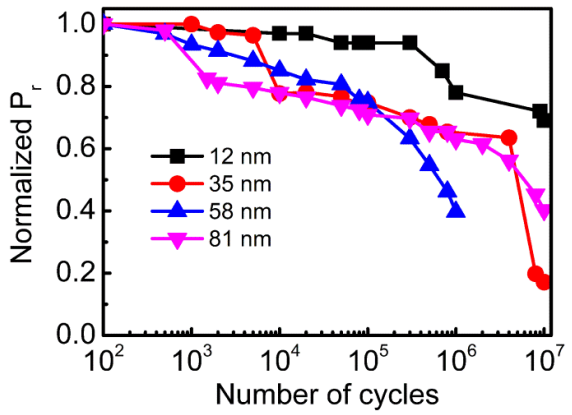

Figure 3. Fatigue characteristics of PVDF homopolymer LB nanofilms at different thicknesses.

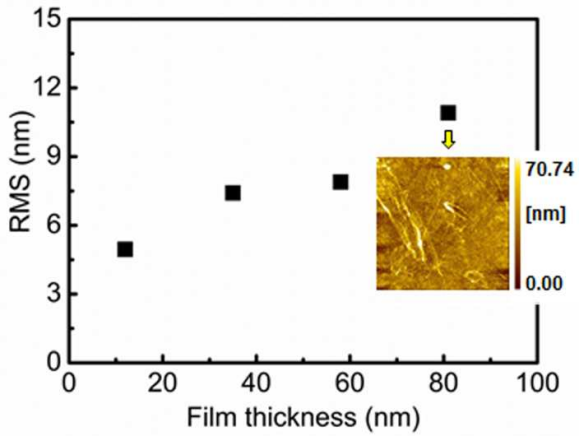

Figure 4. Root-mean square (RMS) surface roughness of PVDF homopolymer LB nanofilms at different thicknesses. The inset figure is an AFM image for an 81-nm-thick film with image size of 10 μm × 10 μm.

In conclusion, ferroelectric polarization switching was investigated in as-prepared PVDF homopolymer LB nanofilms from 12 nm to 81 nm. A P_r of 6.6 μC/cm^2 was obtained in 81-nm-thick PVDF LB nanofilms with no post-treatment such as thermal annealing. That

value is one of the highest ever reported for PVDF micro-/nanofilms. Ferroelectricity was detected first in a 12-nm-thick PVDF homopolymer film, indicating a potential low-voltage application of these PVDF homopolymer nanofilms. The thickness-independent coercive field is attributed to an extrinsic switching mechanism, which is dominated by inhomogeneous domain nucleation and growth. The fatigue properties of the PVDF LB nanofilms provide useful information for elucidating the operation endurance of PVDF nanofilms thinner than 100 nm. Such information is deficient in this research field because of the restriction of film-preparation methods. The high remanent polarization, good fatigue properties, and easy fabrication make PVDF LB nanofilms quite promising for use in non-volatile nanomemories.

Acknowledgements

The work was partially supported by a Grant-in-aid for Scientific Research (B) (24350112) from the Japan Society for the Promotion of Science (JSPS) and Innovative Areas (25102504) from the Ministry of Education, Culture, Sports, Science, and Technology in Japan (MEXT). The work was also supported by the Nano-Macro Materials, Devices and System Research Alliance (MEXT).

Notes and references

1 P. Heremans, G. H. Gelinck, R. Muller, K. J. Baeg, D. Y. Kim and Y. Y. Noh, *Chem. Mater.*, 2011, **23**, 341.

2 (a) T. Kurosawa, Y.-C. Lai, T. Higashihara, M. Ueda, C.-L. Liu and W.-C. Chen, *Macromolecules*, 2012, **45**, 4556; (b) Y.-G. Ko, W. Kwon, H.-J. Yen, C.-W. Chang, D. M.

Kim, K. Kim, S. G. Hahm, T. J. Lee, G.-S. Liou and M. Ree, *Macromolecules*, 2012, **45**, 3749; (c) Y. Li, R. Patil, S. Wei and Z. Guo, *J. Phys. Chem. C*, 2011, **115**, 22863; (d) K.-L. Wang, Y.-L. Liu, J.-W. Lee, K.-G. Neoh and E.-T. Kang, *Macromolecules*, 2010, **43**, 7159.

3 (a) R. J. Tseng, J. Huang, J. Ouyang, R. B. Kaner and Yang, *Nano Lett.*, 2005, **5**, 1077; (b) X. Zhang, J. Zhu, N. Haldolaarachchige, J. Ryu, D. P. Young, S. Wei and Z. Guo, *Polymer*, 2012, **53**, 2109; (c) H. Gu, J. Guo, X. Zhang, Q. He, Y. Huang, H. A. Colorado, N. Haldolaarachchige, H. Xin, D. P. Young, S. Wei and Z. Guo, *J. Phys. Chem. C*, 2013, **117**, 6426; (d) J. Ouyang, C.-W. Chu, C. R. Szmanda, L. Ma and Y. Yang, *Nat. Mater.*, 2004, **3**, 918.

4 (a) Y. J. Shin, S. J. Kang, H. J. Jung, Y. J. Park, I. Bae, D. H. Choi and C. Park, *ACS Appl. Mater. Interfaces*, 2011, **3**, 582; (b) Z. J. Hu, M. W. Tian, B. Nysten and A. M. Jonas, *Nat. Mater.*, 2009, **8**, 62; (c) R. C. G. Naber, C. Tanase, P. W. M. Blom, G. H. Gelinck, A. W. Marsman, F. J. Touwslager, S. Setayesh and D. M. De Leeuw, *Nat. Mater.*, 2005, **4**, 243.

5 K. H. Lee, G. Lee, K. Lee, M. S. Oh and S. Im, *Appl. Phys. Lett.*, 2009, **94**, 093304.

6 (a) H. Kawai, *Jpn. J. Appl. Phys.*, 1969, **8**, 975; (b) A. J. Lovinger, *Science*, 1983, **220**, 1115.

7 A. K. Tripathi, A. van Breemen, J. Shen, Q. Gao, M. G. Ivan, K. Reimann, E. R. Meinders and G. H. Gelinck, *Adv. Mater.*, 2011, **23**, 4146.

8 S. J. Kang, I. Bae, Y. J. Shin, Y. J. Park, J. Huh, S. M. Park, H. C. Kim and C. Park, *Nano Lett.*, 2011, **11**, 138.

9 A. V. Bune, V. M. Fridkin, S. Ducharme, L. M. Blinov, S. P. Palto, A. V. Sorokin, S. G. Yudin and A. Zlatkin, *Nature*, 1998, **391**, 874.

10 M. Li, I. Katsouras, K. Asadi, P. W. M. Blom and D. M. de Leeuw, *Appl. Phys. Lett.*, 2013, **103**, 072903.

11 S. Fujisaki, H. Ishiwara and Y. Fujisaki, *Appl. Phys. Lett.*, 2007, **90**, 162902.

12 (a) T. Miyashita, *Prog. Polym. Sci.*, 1993, **18**, 263; (b) M. Mitsuishi, J. Matsui and T. Miyashita, *J. Mater. Chem.*, 2009, **19**, 325; (c) H. Zhu, M. Mitsuishi and T. Miyashita, *Macromolecules*, 2012, **45**, 9076; (d) M. Ishifuji, M. Mitsuishi and T. Miyashita, *Chem. Commun.*, 2008, 1058.

13 (a) G. Zhu, Z. Zeng, L. Zhang and X. Yan, *Appl. Phys. Lett.*, 2006, **89**, 102905; (b) C. B. Sawyer and C. H. Tower, *Phys. Rev.*, 1930, **35**, 0269.

14 (a) M. Benz and W. B. Euler, *J. Appl. Polym. Sci.*, 2003, **89**, 1093; (b) M. Kobayashi, K. Tashiro and H. Tadokoro, *Macromolecules*, 1975, **8**, 158.

15 R. Gregorio and M. Cestari, *J. Polym. Sci., Part B: Polym. Phys.*, 1994, **32**, 859.

16 W. J. Li, Q. J. Meng, Y. S. Zheng, Z. C. Zhang, W. M. Xia and Z. Xu, *Appl. Phys. Lett.*, 2010, **96**, 192905.

17 K. Urayama, M. Tsuji and D. Neher, *Macromolecules*, 2000, **33**, 8269.

18 T. Nakajima, R. Abe, Y. Takahashi and T. Furukawa, *Jpn. J. Appl. Phys.*, 2005, **44**, L1385.

19 T. Nakajima, Y. Takahashi, S. Okamura and T. Furukawa, *Jpn. J. Appl. Phys.*, 2009, **48**, 09KE04.

20 R. V. Gaynutdinov, S. Mitko, S. G. Yudin, V. M. Fridkin and S. Ducharme, *Appl. Phys. Lett.*, 2011, **99**, 142904.

21 J. J. Li, Q. J. Meng, W. J. Li and Z. C. Zhang, *J. Appl. Polym. Sci.*, 2011, **122**, 1659.

22 (a) B. Helgee and P. Bjellheim, *IEEE Trans.on Electr. Insul.*, 1991, **26**, 1147; (b) H. K. Kim and F. G. Shi, *IEEE Trans. Dielectr. Electr. Insul.*, 2001, **8**, 248.

23 T. Furukawa, T. Nakajima and Y. Takahashi, *IEEE Trans. Dielectr. Electr. Insul.*, 2006, **13**, 1120.

24 M. F. Mai, B. Martin and H. Kliem, *J. Appl. Phys.*, 2011, **110**, 064101